AIP | Applied Physics Letters

Spatially resolved photoluminescence mapping of single CdS nanosheets

H. Rho, K.-Y. Lee, T. B. Hoang, L. V. Titova, A. Mishra, L. M. Smith, H. E. Jackson, J. M. Yarrison-Rice, Y.-J. Choi, K. J. Choi, and J.-G. Park

---

Spatially resolved photoluminescence mapping of single CdS nanosheets

H. Rho[a),b)] and K.-Y. Lee
Department of Physics, Chonbuk National University, Jeonju 561-756, Korea

T. B. Hoang, L. V. Titova, A. Mishra, L. M. Smith, and H. E. Jackson[a),c)]
Department of Physics, University of Cincinnati, Cincinnati, Ohio 45221, USA

J. M. Yarrison-Rice
Physics Department, Miami University, Oxford, Ohio 45056, USA

Y.-J. Choi, K. J. Choi, and J.-G. Park
Nano Materials Research Center, Korea Institute of Science and Technology, Seoul 130-650, Korea

We have utilized spatially resolved low temperature photoluminescence to probe the electronic states and structural symmetries of individual single crystalline CdS nanosheets. Spatially resolved photoluminescence imaging of a single CdS nanosheet reveals a distinctive spectral variation across the nanosheet. We observe A-like exciton states which emit most strongly near the outer edges of the 5 μm wide nanosheet, while B-like exciton states emit most strongly along the center region of the 30 μm long axis of the nanosheet. © 2008 American Institute of Physics.
[DOI: 10.1063/1.2828707]

Semiconductor nanostructures ranging from quantum dots to nanowires to nanosheets have recently attracted considerable attention because of the interesting physics in reduced dimensions, the spatially confined optical and electrical properties, and a plethora of potential applications. In particular, semiconductor nanosheets with good crystallinity are poised to support applications in nanoscale electronic and optoelectronic devices.[1–9] The last few years have seen a variety of different methods used to produce single crystalline nanobelts or nanosheets of materials including ZnO,[10] SnO_2,[11] Ga_2O_3,[12] MgO,[13] ZnS,[14] and CdS.[8,15] CdS nanosheets reported here present significant opportunities for optoelectronic applications with optical switches, high quality field effect transistors, and light emitting diodes recently being demonstrated.[1,5,6,9] Further development of these applications should clearly benefit from a deeper understanding of the nanosheet optical and electronic properties.

In this letter, we use low temperature microphotoluminescence in combination with spatially resolved photoluminescence (PL) spectroscopy to investigate the optical properties of single CdS nanosheets. High resolution transmission electron microscope (HRTEM) images show single crystal, high quality nanosheet growth with hexagonal wurtzite structure. The c axis is seen to be approximately perpendicular to the nanosheet long axis.[16] Using low-temperature polarized PL imaging, we observe high quantum efficiency emission corresponding to A- and B-hole band excitons and, through polarization analysis, we can determine the orientation of the c axis for a particular single CdS nanosheet.[16] Spatially resolved PL imaging of single nanosheets reveals striking PL intensity and line shape variation along the length and width of a nanosheet. This implies some variation in uniformity, strain, or defects across the nanosheet. All nanosheet dimensions (~50 nm thickness, ~5 μm width, and ~30 μm length) are much larger than the CdS Bohr exciton radius

(6 nm) and, thus, no quantum confinement effects are expected. CdS nanosheets were grown by pulsed laser deposition using the vapor-phase transport method.[17]

The size and shape of the nanosheets are quite uniform. The upper inset in Fig. 1 shows a high-magnification scanning electron microscopy (SEM) image of a single nanosheet. The surface of the nanosheet is curved and smooth with a uniform thickness over the larger surface area. To measure single structures, the nanosheets were dispersed from the growth substrate into an ethanol solution and then deposited on a silicon substrate; the as-grown nanosheets (see lower inset of Fig. 1) are held flat to the substrate by van der Waals' forces.

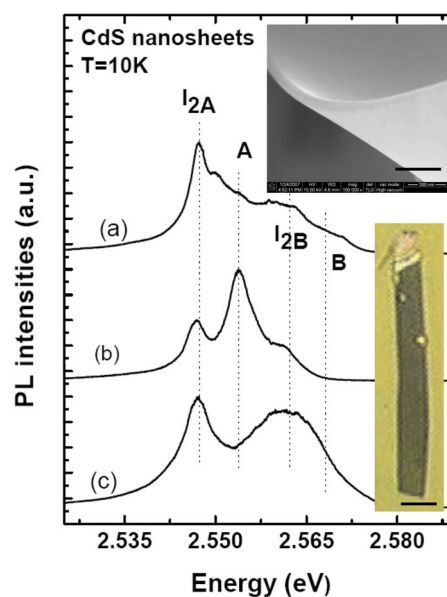FIG. 1. (Color online) Normalized photoluminescence spectra from three different single nanosheets. Upper inset is a high-magnification SEM image of a single nanosheet (dark line = 300 nm) and lower inset is an optical micrograph of the ~5 × 30 μm² nanosheet.

[a)]Authors to whom correspondence should be addressed.
[b)]Electronic mail: rho@chonbuk.ac.kr.
[c)]Electronic mail: howard.jackson@uc.edu.

The crystallinity and structure of individual CdS nanosheets were investigated by HRTEM which showed a highly crystalline wurtzite structure with the *c* axis nearly perpendicular to the long axis of the CdS nanosheet. Other CdS nanosheets, however, were found to have the *c* axis at other orientations relative to the long axis of the nanosheet.[16] Low temperature PL from a single nanosheet was collected using a $50\times/0.5$ numerical aperture long working length microscope objective, which was also used to focus the 458 nm line of a cw Argon ion laser. The PL was dispersed by a triple spectrometer working in subtractive mode, and detected by a 2000×800 pixel liquid nitrogen-cooled charge-coupled device (CCD) detector. Spectra were measured with the excitation laser circularly polarized while the emission passed through a linear polarization analyzer aligned parallel to the long axis of each nanosheet. All measurements were conducted at 15 K.

In Fig. 1, we show typical low temperature cw PL spectra of three different single CdS nanosheets. The PL intensity from each nanosheet is strong, indicating emission from the CdS nanosheet occurs with high quantum efficiency. This emission is entirely near the CdS band edge and, unlike previous CdS nanosheet low temperature PL measurements, no evidence for donor-acceptor or surface related emission was seen at lower energies.[4,18] We find that each of the nanosheets displays a narrow peak [full width at half maxi-

mum (FHWM) ~4 meV] at 2.547 eV and a broader response (FHWM ~11 meV) at higher energies near 2.563 eV. The broad response varies in energy (2.553–2.571 eV) from sheet to sheet and can also display internal spectral structure indicating contributions from more than one exciton state. Recall that in the wurtzite structure the *p*-like hole bands are split so that there may be three excitons labeled *A*, *B*, and *C*. The lower energy peak we observe is situated near the spectral line observed in bulk CdS associated with the I_{2A} line at 2.547 eV, which results from recombination of an *A* exciton bound to a neutral donor. The *A* free exciton should be some 6 meV higher in energy at 2.553 eV.[19,20] The higher energy broad peak is in the region of the I_{2B} line at 2.563 eV, resulting from recombination of a *B* exciton bound to a neutral donor. The *B* free exciton line is expected at 2.569 eV.

To gain more insight into the nature of these two lines, which exist in the *A*- and *B*-excitonic regions for CdS, we use slit-confocal microscopy to directly image an entire CdS nanosheet with 1.5 μm spatial resolution. This technique is described in more detail in Hewaparakrama *et al.*[21] The nanosheet, with its entire area excited by a defocused laser, is scanned underneath the fixed microscope objective, and a series of two-dimensional CCD spectral images are collected. Ultimately, a large three-dimensional data set is acquired, which has full 500 point spectra at every spatial point
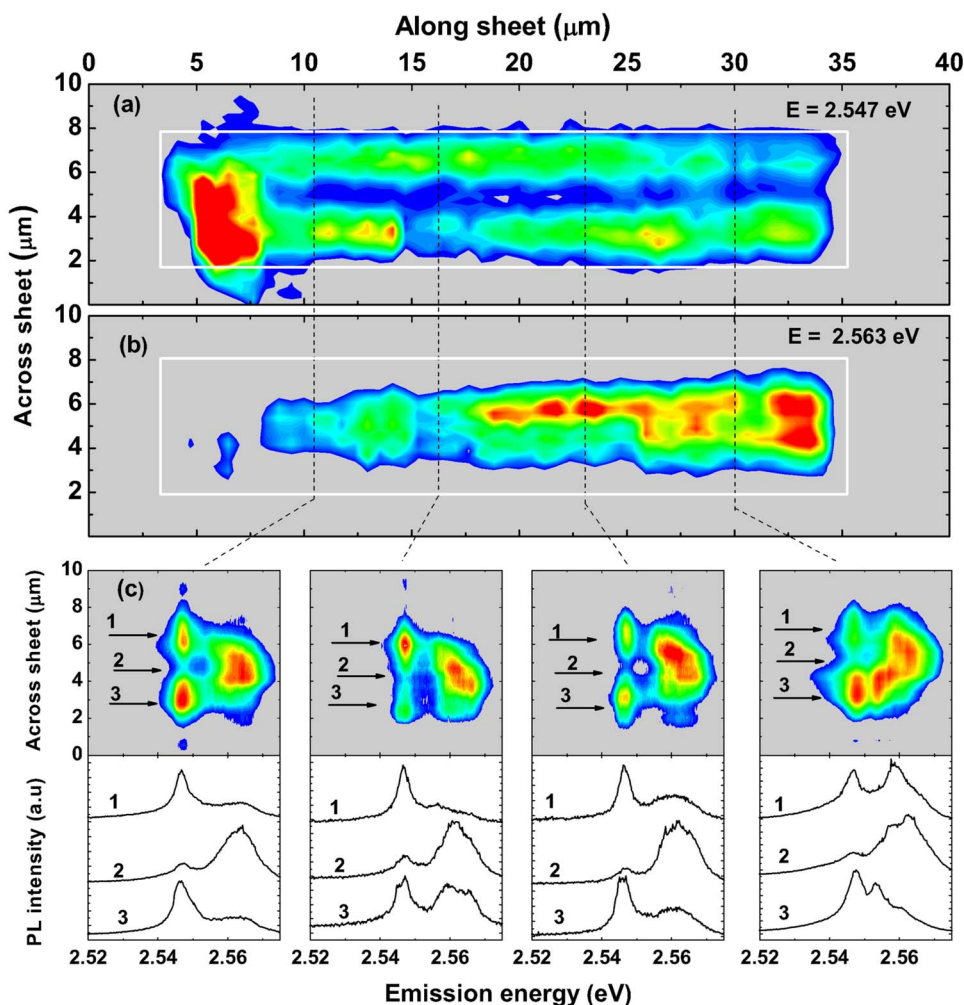

FIG. 2. (Color online) (a) PL image of a single nanosheet at energies of 2.547 eV and (b) at 2.563 eV (white box shows approximate outline of this nanosheet) and (c) two-dimensional images and photoluminescence spectra taken at different positions along a single nanosheet shown by the dashed lines.

along and across the nanosheet. In this way, it becomes possible to correlate spectral and spatial features of the nanosheet.

We present in detail such spatially resolved PL measurements of nanosheet 3 in Fig. 2. This nanosheet is ~5 μm wide ×30 μm long. Figures 2(a) and 2(b) show PL images of this nanosheet at two photon energies (2.547 and 2.563 eV) associated with the two well-resolved spectral peaks seen for the nanosheet in Fig. 1(c) for nanosheet 3. These spatial maps aredisplayed as false-color images on a logarithmic scale with red used for the most intense emission from the nanosheet. In these images, the vertical and horizontal axes denote the spatial positions across the width and along the length of the nanosheet, respectively. Quite unexpectedly, we find that, as displayed in Fig. 2(a), the peak at lower energy emits most strongly along the edges of the nanosheet, while, as seen in Fig. 2(b), the higher energy peak emits most strongly at the center of the nanosheet. From both the spatial maps and the selected area PL spectra, we observe that the emissions which we assign to the I_{2A} and I_{2B} donor bound excitons emit in different spatial regions of the nanosheet.

A plausible explanation of this distinctive spatial separation may be the spatial distribution of stress in this system. SEM images show that stress induces the curl of the nanosheets and that the flattening onto a substrate for optical measurement may induce stress. Recent Raman measurements[22] also indicate the presence of significant stress in the nanosheets. A spatial gradient of stress from the center to the edge of the nanosheet would affect the *A* and *B* excitons differentially,[23] resulting in potential minima either along the edge or in the center for the *A*- and *B*-valence band excitons, respectively. More detailed measurements with the higher spatial resolution offered by use of a solid immersion lense are clearly required to interpret these results.[21,24]

To display more detailed spectral information along the nanosheet, we extract the original CCD spectral maps from the full three-dimensional data set. These spectral maps, shown in the bottom row of images of Fig. 2, display the PL spectra as a function of position across the width of the nanosheet. Four such spectral maps are shown at positions along the length of the nanosheet, as shown by the dashed lines. From these four spectral maps in the bottom row of Fig. 2(c) a number of general observations can be made. We see that in every cross section the spectral peak at 2.547 eV appears most intensely at the edges of the nanosheet. Moreover, the broader peak observed at the higher energy of ~2.563 eV predominantly emits along the center of the nanosheet, but the spectral position of this peak appears to vary both in energy and position from slice to slice along the nanosheet. Below each spectral map are shown PL emission spectra extracted from three different vertical locations as indicated by the horizontal arrows in each spectral map. From such spatially resolved spectra, we can see that the PL spectrum not only changes when crossing the width of the nanosheet, but also depends on position along the length of

the nanosheet. Other nanosheets showed similar PL imaging results.

In conclusion, we have shown that catalyst-assisted vapor phase growth of CdS nanosheets with large width-to-thickness aspect ratios results in high quality hexagonal wurtzite single crystals which display intense band edge emission at low temperatures with no noticeable defect emission at lower energies. Both *A*- and *B*-related exciton emissions are observed, with spatially resolved PL spectra of single nanosheets showing striking spatial variability of the intensity of these lines across the nanosheet indicating the influence of strains. Finally, we have shown how spatially resolved low temperature PL spectroscopy can rapidly characterize the electronic and crystalline structure of nanosheets in a nondestructive way.

[1]X. F. Duan, C. M. Niu, V. Sahi, J. Chen, J. W. Parce, S. Empedocles, and J. L. Goldman, Nature (London) **425**, 274 (2003).
[2]Z. L. Wang, Annu. Rev. Phys. Chem. **55**, 159 (2004).
[3]L. Weifeng, J. Chong, J. Chuangui, Y. Lianzeng, C. Weili, and L. Xiaoguang, J. Cryst. Growth **269**, 304 (2004).
[4]W. Chunrui, K. M. Ip, S. K. Hark, and L. Quan, J. Appl. Phys. **97**, 054303 (2005).
[5]T. Gao, Q. H. Li, and T. H. Wang, Appl. Phys. Lett. **86**, 173105 (2005).
[6]R. M. Ma, L. Dai, H. B. Huo, W. Q. Yang, G. G. Qin, P. H. Tan, C. H. Huang, and J. Zheng, Appl. Phys. Lett. **89**, 203120 (2006).
[7]D. H. L. Ng, W. Yu, and C. Y. To, Mater. Lett. **60**, 1151 (2006).
[8]Z. Q. Wang, J. F. Gong, J. H. Duan, H. B. Huang, S. G. Yang, X. N. Zhao, R. Zhang, and Y. W. Du, Appl. Phys. Lett. **89**, 033102 (2006).
[9]R. M. Ma, L. Dai, and G. G. Qin, Nano Lett. **7**, 868 (2007).
[10]P. Z. Wei, D. Z. Rong, and W. Z. Lin, Science **291**, 1947 (2001).
[11]S. H. Sun, G. W. Meng, G. X. Zhang, T. Gao, B. Y. Geng, L. D. Zhang, and J. Zuo, Chem. Phys. Lett. **376**, 103 (2003).
[12]Z. R. Dai, Z. W. Pan, and Z. L. Wang, J. Phys. Chem. B **106**, 902 (2002).
[13]R. Ma and Y. Bando, Chem. Phys. Lett. **370**, 770 (2003).
[14]Y.-C. Zhu, Y. Bando, and D.-F. Xoe, Appl. Phys. Lett. **82**, 1769 (2003).
[15]L. Chen, L. Zengtao, and Y. Yong, Nanotechnology **17**, 1851 (2006).
[16]T. B. Hoang, H. Rho, L. V. Titova, A. Mishra, K.-Y. Lee, J. M. Yarrison-Rice, H. E. Jackson, L. M. Smith, Y.-J. Choi, K. J. Choi, and J.-G. Park "Polarized photoluminescence and time-resolved photoluminescence from single CdS nanosheets," (unpublished).
[17]M. H. Huang, Y. Y. Wu, H. Feick, N. Tran, E. Weber, and P. D. Yang, Adv. Mater. (Weinheim, Ger.) **13**, 113 (2001).
[18]K. M. Ip, C. R. Wang, Q. Li, and S. K. Hark, Appl. Phys. Lett. **84**, 795 (2004).
[19]D. G. Thomas and J. J. Hopfield, Phys. Rev. **128**, 2135 (1962).
[20]J. J. Hopfield and D. G. Thomas, Phys. Rev. **122**, 35 (1961).
[21]K. P. Hewaparakrama, A. Wilson, S. Mackowski, H. E. Jackson, L. M. Smith, G. Karczewski, and J. Kossut, Appl. Phys. Lett. **85**, 5463 (2004).
[22]K.-Y. Lee, J.-R. Lim, H. Rho, Y.-J. Choi, K. J. Choi, and J.-G. Park, Appl. Phys. Lett. **91**, 201901 (2007).
[23]D. W. Langer, R. N. Euwema, K. Era, and T. Koda, Phys. Rev. B **2**, 4005 (1970).
[24]S. Mackowski, T. Gurung, H. E. Jackson, L. M. Smith, G. Karczewski, and J. Kossut, Appl. Phys. Lett. **87**, 072502 (2005).